AIMS Mathematics, 11(11): 37289–37310.
DOI: 10.3934/math.20261442
Received: 15 May 2026
Revised: 04 October 2026
Accepted: 26 October 2026
Published: 11 November 2026

http://www.aimspress.com/journal/Math

Research article

Theoretical and computational aspects for the nonlinear time-fractional Allen-Cahn model using two efficient approaches

Hegagi Mohamed Ali[1,2,*], **and Wedad Albalawi**[3]

[1] Department of Mathematics, College of Science, University of Bisha, Bisha 61922, Saudi Arabia
[2] Department of Mathematics, Faculty of Science, Aswan University, Aswan 81528, Egypt
[3] Department of Mathematical Sciences, College of Science, Princess Nourah bint Abdulrahman University, P.O. Box 84428, Riyadh 11671, Saudi Arabia

* **Correspondence:** Email: he.ahmed@ub.edu.sa, hegagi_math@aswu.edu.eg.

Abstract: This research investigates an approximate solution to the nonlinear temporal-fractional Allen-Cahn equation (A-CE), a fundamental model for the dynamics of phase separation in binary alloys and pattern formation in physical systems. The conventional integer-order A-CE is extended to a fractional-order model employing the Caputo fractional derivative to capture long-range dependencies and memory effects. The modified generalized Mittag-Leffler function method (MGMLFM) and the Temimi-Ansari method (TAM) are employed as two analytical methods to achieve the study's goal. These methods provide a rapidly convergent solution to the known exact solution. Additionally, a comparison between the error analysis of these methods and the results obtained from other methods found in the literature, such as the Elzaki iterative transform method (EITM), homotopy perturbation method (HPM), new iterative transform method (NITM), Laplace residual power series method (LRPSM), and homotopy analysis method (HAM), to verify the accuracy of both methods. The simulation results are displayed in 2D and 3D plots and data tables. The outcomes confirm that the approximate solution when $\alpha \to 1$ converges very closely with the exact solution. The absolute errors are competitive with, and in many tested cases smaller than, those of other published methods; however, the comparison is not uniformly favorable, and the relative accuracy depends on the specific space–time point and fractional order.The numerical results indicate that the relative accuracy of the MGMLFM and the HAM varies across the considered space-time points and fractional orders.The proposed framework establishes both the MGMLFM and the TAM as powerful tools to analyze complex fractional-order nonlinear systems that emerge in materials science and engineering.

Keywords: Allen-Cahn equation; Caputo fractional derivative; partial differential equations; Mittag-Leffler function; analytical approximate solutions
Mathematics Subject Classification: 35R11, 33E12, 35C10, 65M70, 74H10

1. Introduction

The Allen-Cahn equation (A-CE) is an essential partial differential equation (PDE) in materials science and mathematical physics [1, 2]. It was first used to explain the behavior of anti-phase barriers during the phase separation process in binary alloys. In systems going through phase transitions, the equation serves as a prototype to simulate the evolution of an order parameter, which stands for the local state of the system, such as the concentration of a single component in a binary mixture [3,4]. Over the years, the A-CE has been used in fields other than materials science, such as biology, image processing, and pattern creation research. It is a useful tool for comprehending the dynamics of phase transitions and interfacial phenomena in a variety of physical and biological systems because of its simplicity and rich mathematical structure [5–7]. Recent developments provide several promising directions to extend time-fractional Allen-Cahn models. Recent adaptive numerical developments for the A-CE also include spatially adaptive schemes on curved surfaces and adaptive narrow-band strategies to efficiently resolve moving interfaces [8]. In addition, adaptive time-stepping techniques have been developed to improve the computational efficiency and temporal accuracy of Allen-Cahn simulations, particularly in regimes that involve rapid phase evolution [9]. Another promising extension is the incorporation of variable mobility into the Allen-Cahn framework [10]. These developments suggest several possible future extensions of the present study, including the formulation of time-fractional Allen-Cahn equations on curved surfaces, the incorporation of adaptive spatial and temporal discretizations, and the consideration of variable-mobility fractional phase-field models.

While classical PDEs such as the A-CE are powerful tools to model phenomena such as heat conduction, fluid dynamics, and wave propagation, they rely on integer-order derivatives that assume instantaneous responses and local interactions. However, many real-world models—including anomalous diffusion, viscoelastic materials, and biological processes—show memory effects and long-range dependencies that integer-order models cannot adequately capture [11]. Fractional differential equations (FDEs), which generalize classical derivatives to non-integer orders, offer a natural framework to incorporate such nonlocal effects [12, 13]. Therefore, the fractional calculus (FC) framework provides an effective mathematical tool to model these phenomena more accurately, and has received considerable attention due to its ability to describe complex systems with greater accuracy and flexibility [14]. Consequently, extending the A-CE into a time-fractional form offers a more realistic description of phase transition dynamics.

It is widely acknowledged that obtaining accurate solutions to PDEs is a major challenge, whether through numerical or analytical methods. As a result, researchers have focused on developing innovative methods to get approximate solutions for these equations. Still, there is no single method capable of solving all types of PDEs; this led to the consideration of various approaches in the literature for dealing with nonlinear PDEs. Examples of such approaches include the homotopy analysis method [15], variational iteration method [16], residual power series transform method [17], finite difference method [18], Sumudu transform method [19], Adomian decomposition method [20], finite element method [21], homotopy perturbation method [22], and numerous other techniques (for instance, see [23–25]).

The modified generalized Mittag-Leffler function method (MGMLFM) generates a rapidly convergent series solution directly expressed in terms of the Mittag-Leffler function, which by its very nature embodies the memory effects and long-range dependencies introduced by the Caputo

fractional derivative (CFD). Its main advantage lies in providing extremely accurate solutions with very small absolute errors and minimal computational efforts, often outperforming current methods in the literature. However, the MGMLFM requires careful handling of nonlinear terms through He's polynomials and the inference of recurrence relations, which can become algebraically intensive for strongly nonlinear or high-order problems. On the other hand, the Temimi-Ansari method (TAM) provides a simpler iterative framework that avoids the calculation of complicated polynomials or recurrence coefficients. It is straightforward to apply, especially when the initial condition is considered to be the first approximation, and it offers credible accuracy with fewer analytical operations. Nevertheless, the TAM may require a greater number of iterations to realize the same accuracy as the MGMLFM, and its convergence is generally slower for equations with strong nonlinearity. By comparing these two suggested methods side-by-side, this study not only reveals their effectiveness but also supplies practical insight into selecting a convenient analytical tool based on the trade-off between accuracy, computational effort, and algebraic complexity.

The motivation of this study is to extend the classical A-CE to a time-fractional form using the CFD, which enables the model to capture memory-dependent phase evolution, and to introduce the MGMLFM and TAM as a powerful analytical tools for obtaining highly accurate approximate solutions to the following temporal-fractional A-CE.

We consider the following time-fractional A-CE on the infinite domain $x \in \mathbb{R}$:

$$\frac{\partial^\alpha \mathscr{W}(x,t)}{\partial t^\alpha} - \frac{\partial^2 \mathscr{W}(x,t)}{\partial x^2} + \mathscr{W}^3(x,t) - \mathscr{W}(x,t) = 0, \tag{1.1}$$

under the appropriate initial condition (IC)

$$\mathscr{W}(x,0) = \mathscr{W}_0(x), \tag{1.2}$$

where $\frac{\partial^\alpha}{\partial t^\alpha}$ is Caputo partial fractional derivative. To the best of our knowledge, the application of the proposed methods to this equation has not been fully explored in the literature.

The main contributions of this study are summarized in the following points;

- Deriving approximate analytical solutions for the time-fractional A-CE using MGMLFM and comparing them with those obtained via the TAM;
- Validating the accuracy of the proposed methods against exact solutions and several existing techniques homotopy perturbation method (HPM), new iterative transform method (NITM), Elzaki iterative transform method (EITM), homotopy analysis method (HAM), Laplace residual power series method (LRPSM) through comprehensive numerical simulations and error tables;
- Demonstrating that as the fractional order α approaches 1, the approximate solutions smoothly converge to the exact integer-order solution; and
- Showing that proposed methods achieve significantly smaller absolute errors compared to other published methods, establishing it as a superior analytical tools.

A significant novelty of our work is the side-by-side comparison of two fundamentally different analytical approaches—MGMLFM (series expansion based on Mittag-Leffler functions) and TAM (iterative fractional integration)—applied to the same fractional Allen-Cahn problem. Therefore, the novelty of the present work does not lie in introducing the original Temimi–Ansari iterative method, which was previously established [26]. Rather, the present study focuses on its formulation

and implementation for the time-fractional A-CE through a fractional-integral iterative construction. The resulting formulation is investigated in conjunction with the MGMLFM framework and is evaluated for representative fractional orders. Thus, the established iterative principle is distinguished from its fractional Allen-Cahn application developed and analyzed in the present study.This study provides a comprehensive accuracy comparison against five existing methods—HPM, NITM, EITM, LRPSM, and HAM—in the literature [5–7]. The results demonstrate that both the MGMLFM and the TAM achieve significantly smaller absolute errors (orders of magnitude smaller) compared to these established techniques. This extensive comparative validation establishes the superiority of the proposed methods in terms of accuracy. Therefore, our work introduces new analytical tools to the existing toolkit for this important phase-field model and offers an attractive alternative to more complex methods.

The organization of this paper is as follows: in Section 2, we introduce fundamental preliminaries for FC which assist us in carrying out this study; Section 3 explains the generic algorithm of the proposed methods; Section 4 is devoted to gaining the approximate solution for the time-fractional nonlinear A-CE Eq (1.1) under the appropriate IC using the MGMLFM in Subsection 4.1 and applying the TAM in Subsection 4.2, and a numerical simulation of the acquired results is presented; and the outcomes of this research are concluded in Section 5.

2. Preliminaries

Fundamental concepts and terminology are introduced in this section to support and advance this research [27, 28].

Definition 2.1. *The Riemann-Liouville fractional integral is defined as follows:*

$$ {}_0\mathcal{I}_t^{\alpha}\mathcal{S}(x,t) = \begin{cases} \frac{1}{\Gamma(\alpha)}\int_0^t (t-\zeta)^{\alpha-1}\mathcal{S}(x,\zeta)d\zeta, & t>0, \quad \alpha>0, \\ \mathcal{S}(x,t), & \alpha=0. \end{cases} $$

The following is satisfied:

$$ {}_0\mathcal{I}_t^{\alpha}t^{\beta} = \frac{\Gamma(\beta+1)}{\Gamma(\beta+\alpha+1)}t^{\beta+\alpha}. $$

Definition 2.2. *The CFD for a function $\mathcal{S}(x,t)$ such that its n-th partial derivative with respect to t is defined by the following:*

$$ \frac{\partial^{\alpha}\mathcal{S}(x,t)}{\partial t^{\alpha}} = \begin{cases} \frac{1}{\Gamma(n-\alpha)}\int_0^t (t-\beta)^{n-\alpha-1}\frac{\partial^n\mathcal{S}(x,\beta)}{\partial\beta^n}d\beta, & for \quad n-1<\alpha<n; n\in\mathbb{N}, \\ \frac{\partial^n\mathcal{S}(x,t)}{\partial t^n}, & for \quad \alpha=n\in\mathbb{N}. \end{cases} $$

For $t>0$ and $0<\alpha<1$, the CFD of a power function is given by the following:

$$ {}_0^C\mathcal{D}_t^{\alpha}t^{\beta} = \begin{cases} 0, & \beta=0, \\ \frac{\Gamma(\beta+1)}{\Gamma(\beta+1-\alpha)}t^{\beta-\alpha}, & \beta>0. \end{cases} $$

Theorem 2.1. *Let $\mathscr{S}(x,t)$ be a differentiable function and $n-1<\alpha<n$ and $n\in\mathbb{N}$; then,*

$$\begin{aligned} {}_0^C\mathcal{D}_t^{\alpha}\,{}_0\mathcal{I}_t^{\alpha}\mathscr{S}(x,t) &= \mathscr{S}(x,t), \\ {}_0\mathcal{I}_t^{\alpha}\,{}_0^C\mathcal{D}_t^{\alpha}\mathscr{S}(x,t) &= \mathscr{S}(x,t)-\sum_{\kappa=0}^{n-1}\frac{\partial^{\kappa}\mathscr{S}(x,t)}{\partial t^{\kappa}}|_{t=0}\frac{t^{\kappa}}{\kappa!}. \end{aligned}$$

Definition 2.3. *The Mittag-leffler function $E(\cdot)$ is defined as follows:*

$$E_{\alpha}(t)=\sum_{\kappa=0}^{\infty}\frac{t^{\kappa}}{\Gamma(\kappa\alpha+1)},\quad \alpha>0.$$

Lemma 2.1. *The CFD of $E_{\alpha}(At^{\alpha})$ is given by the following:*

$${}_0^C\mathcal{D}_t^{\alpha}E_{\alpha}(At^{\alpha})=\sum_{n=0}^{\infty}\frac{A^{n+1}t^{n\alpha}}{\Gamma(n\alpha+1)}=AE_{\alpha}(At^{\alpha}).$$

Theorem 2.2. *[29] Let $\mathscr{S}(x,t)=\sum_{\kappa=0}^{\infty}\theta^{\kappa}\mathscr{S}_{\kappa}(x,t)$; then, the nonlinear operator $N(\cdot)$ is*

$$N(\mathscr{S})=\sum_{n=0}^{\infty}\Big(\frac{1}{n!}\frac{\partial^n}{\partial\theta^n}\Big[N\Big(\sum_{\kappa=0}^{n}\theta^{\kappa}\mathscr{S}_{\kappa}\Big)\Big]_{\theta=0}\Big)\theta^n.$$

3. Analysis of proposed methods

In this section, we present the fundamental algorithm of the MGMLFM and TAM to solve the general form of fractional PDEs.

Let the general form of a nonlinear fractional PDE be considered as follows:

$${}_0^C\mathcal{D}_t^{\alpha}\mathscr{S}(x,t)=L(\mathscr{S}(x,t))+N(\mathscr{S}(x,t)), \tag{3.1}$$

with IC

$$\mathscr{S}(x,0)=G(x), \tag{3.2}$$

where L and N are linear and nonlinear operators, respectively.

3.1. Analysis of MGMLFM

The procedure of the MGMLFM to solve the fractional PDE (3.1) is presented. Therefore, the solution of Eq (3.1) is suggested as follows:

$$\mathscr{S}(x,t)=\sum_{n=0}^{\infty}G(x)\lambda_n(x)\frac{t^{n\alpha}}{\Gamma(n\alpha+1)}, \tag{3.3}$$

where $\lambda_n(x)$ are independent coefficient functions to be determined, with $\lambda_0(x)=1$, and $G(x)$ is an auxiliary function. Applying the CFD to Eq (3.3), and using the following power-function property for $0<\alpha<1$,

$${}_0^C\mathcal{D}_t^{\alpha}\Big(\frac{t^{n\alpha}}{\Gamma(n\alpha+1)}\Big)=\frac{t^{(n-1)\alpha}}{\Gamma((n-1)\alpha+1)},n\geq 1.$$

Hence,

$$ {}_0^C\mathcal{D}_t^\alpha \mathcal{S}(x,t) = \sum_{n=0}^{\infty} G(x)\lambda_{n+1}(x)\frac{t^{n\alpha}}{\Gamma(n\alpha+1)}. $$

Therefore, Eq (3.1) can be rewritten as follows:

$$ \sum_{n=0}^{\infty} G(x)\lambda_{n+1}(x)\frac{t^{n\alpha}}{\Gamma(n\alpha+1)} = L(\sum_{n=0}^{\infty} G(x)\lambda_n(x)\frac{t^{n\alpha}}{\Gamma(n\alpha+1)}) + N(\sum_{n=0}^{\infty} G(x)\lambda_n(x)\frac{t^{n\alpha}}{\Gamma(n\alpha+1)}). \tag{3.4} $$

Consequently, the $L(\cdot)$ is expressed as follows:

$$ L(\mathcal{S}(x,t)) = \sum_{n=0}^{\infty} L\Big(G(x)\lambda_n(x)\frac{t^{n\alpha}}{\Gamma(n\alpha+1)}\Big). \tag{3.5} $$

Following He's polynomials [30] and Theorem 2.2, the $N(\cdot)$ is given as follows:

$$ N(\mathcal{S}(x,t)) = N(\mathcal{S}_0(x,t)) + \sum_{n=1}^{\infty}\Big[N\Big(\sum_{i=0}^{n}\mathcal{S}_i(x,t)\Big) - N\Big(\sum_{i=0}^{n-1}\mathcal{S}_i(x,t)\Big)\Big]. \tag{3.6} $$

Utilizing Eqs (3.5) and (3.6) in Eq (3.4), we get the recurrence relation to identify λ and the general solution of Eq (3.1).

3.2. Analysis of TAM

The TAM is an established semi-analytical iterative technique originally introduced by Temimi and Ansari for solving nonlinear differential problems [26]. The basic idea of the TAM is to construct a sequence of successive approximations in which the governing equation is treated iteratively without requiring restrictive assumptions for the nonlinear terms. In the present study, the iterative scheme of TAM is adapted to the time-fractional A-CE. In contrast to the original formulation, the temporal derivative is fractional and is therefore treated through the corresponding fractional integral operator. Accordingly, the successive approximations are constructed in a fractional-integral framework, while the nonlinear reaction term is iteratively evaluated. This adaptation allows the TAM concept to be employed for the fractional Allen-Cahn model.In this subsection, the framework of the TAM to solve the nonlinear fractional PDE Eq (3.1) is presented. Apply the fractional integral operator ${}_0\mathcal{I}_t^\alpha$ to both sides of Eq (3.1). Using the property of the Caputo derivative given in Theorem 2.1, we obtain the following:

$$ \mathcal{S}(x,t) = G(x) + {}_0\mathcal{I}_t^\alpha\left(L(\mathcal{S}(x,t)) + N(\mathcal{S}(x,t))\right). $$

The TAM defines an iterative scheme as follows:

$$ \mathcal{S}_{n+1}(x,t) = G(x) + {}_0\mathcal{I}_t^\alpha\left(L(\mathcal{S}_n(x,t)) + N(\mathcal{S}_n(x,t))\right), \quad n \geq 0. $$

The initial approximation is chosen as the IC:

$$ \mathcal{S}_0(x,t) = G(x). $$

Thus, the first iterative becomes the following:

$$ \mathcal{S}_1(x,t) = G(x) + {}_0\mathcal{I}_t^\alpha\left(L(\mathcal{S}_0(x,t)) + N(\mathcal{S}_0(x,t))\right). $$

The next iteration is determined by the following:

$$\mathscr{S}_2(x,t) = G(x) + {}_0\mathcal{I}_t^{\alpha}\left(L(\mathscr{S}_1(x,t)) + N(\mathscr{S}_1(x,t))\right).$$

Then, the approximate solution is obtained as follows:

$$\mathscr{S}_{\text{approx}}(x,t) = \lim_{n\to\infty} \mathscr{S}_n(x,t) \approx \mathscr{S}_M(x,t),$$

for a sufficiently large M.

3.3. Convergence and error estimator analysis

Here, we establish a conditional convergence result for the fractional series representation used in the proposed analytical procedures. The result is formulated in a Banach space and distinguishes the convergence of the constructed series from the subsequent identification of its limit with a solution of the governing fractional PDE. Let

$$\Omega_T = D \times [0,T],$$

where $D \subseteq \mathbb{R}$ denotes the spatial domain and $T > 0$ is fixed. For the problem considered in this study, the fractional order satisfies $0 < \alpha < 1$. Let

$$\mathbb{B} = C_b(\Omega_T)$$

denote the space of bounded continuous functions on Ω_T, equipped with the supremum norm

$$\|v\|_{\mathbb{B}} = \sup_{(x,t)\in\Omega_T} |v(x,t)|.$$

Consider the series

$$S(X,t) = \sum_{n=0}^{\infty} V_n(X,t),$$

where V_n denotes the n-th series component. The corresponding N-th partial sum is defined by

$$S_N(X,t) = \sum_{k=0}^{N} V_k(X,t).$$

Consequently,

$$S_N - S_{N-1} = V_N, \qquad N \geq 1,$$

with the series components V_n, the partial sums S_N, and the increments $S_N - S_{N-1}$.

Theorem 3.1. *Let $\mathbb{B} = C_b(\Omega_T)$ be the Banach space defined above. Suppose that the series components $V_n \in \mathbb{B}$ satisfy*

$$\|V_{n+1}\|_{\mathbb{B}} \leq q\|V_n\|_{\mathbb{B}}, \qquad n \geq 0,$$

for some constant $0 < q < 1$. Then, the sequence of partial sums

$$S_N = \sum_{k=0}^{N} V_k$$

is a Cauchy sequence in $\mathbb{B}$. Consequently, the series $\sum_{n=0}^{\infty} V_n$ converges in $\mathbb{B}$ to a limit $S \in \mathbb{B}$.

Proof. For $N > M \geq 0$,

$$S_N - S_M = \sum_{k=M+1}^{N} V_k.$$

Hence, by the triangle inequality,

$$\|S_N - S_M\|_{\mathbb{B}} \leq \sum_{k=M+1}^{N} \|V_k\|_{\mathbb{B}}.$$

From the assumed geometric estimate,

$$\|V_k\|_{\mathbb{B}} \leq q^{k-M}\|V_M\|_{\mathbb{B}},$$

and therefore

$$\|S_N - S_M\|_{\mathbb{B}} \leq \|V_M\|_{\mathbb{B}} \sum_{j=1}^{N-M} q^j.$$

Since $0 < q < 1$,

$$\|S_N - S_M\|_{\mathbb{B}} \leq \frac{q}{1-q}\|V_M\|_{\mathbb{B}}.$$

Alternatively, iterating the contraction estimate from V_0 gives

$$\|V_k\|_{\mathbb{B}} \leq q^k\|V_0\|_{\mathbb{B}},$$

and consequently

$$\|S_N - S_M\|_{\mathbb{B}} \leq \frac{q^{M+1}}{1-q}\|V_0\|_{\mathbb{B}}.$$

Because $0 < q < 1$,

$$\lim_{M\to\infty} \frac{q^{M+1}}{1-q}\|V_0\|_{\mathbb{B}} = 0.$$

Hence, $\{S_N\}$ is a Cauchy sequence in the Banach space $\mathbb{B}$. By completeness of $\mathbb{B}$, there exists $S \in \mathbb{B}$ such that

$$S_N \to S \quad \text{in } \mathbb{B}.$$

The identification of S with a solution of the governing fractional PDE requires the additional regularity and limit-passage conditions stated below. □

Proposition 3.1. *Let $S_N \to S$ uniformly on Ω_T. In addition, assume the following:*

- *$S_N \to S$ in a function space for which the required spatial derivatives satisfy*

$$\partial_{xx} S_N \to \partial_{xx} S;$$

- *the CFD exist and*

$${}_0^C D_t^\alpha S_N \to {}_0^C D_t^\alpha S;$$

- *the nonlinear term is continuous under the convergence considered, so that*

$$S_N^3 \to S^3;$$

- *the initial condition is preserved in the limit:*

$$S_N(x,0) \to S(x,0) = \mathscr{W}_0(x).$$

If each partial approximation satisfies the governing equation up to a residual R_N satisfying

$$\|R_N\|_{\mathbb{B}} \to 0,$$

then the limiting function S satisfies

$$ {}_0^C D_t^\alpha S - \frac{\partial^2 S}{\partial x^2} + S^3 - S = 0,$$

together with $S(x,0) = \mathscr{W}_0(x)$.

Theorem 3.2. *Under the assumptions of Theorem 3.1, let*

$$S = \sum_{n=0}^{\infty} V_n \qquad \text{and} \qquad S_m = \sum_{n=0}^{m} V_n.$$

Then, the truncation error satisfies the following:

$$\|S - S_m\|_{\mathbb{B}} \le \frac{q^{m+1}}{1-q}\|V_0\|_{\mathbb{B}}.$$

Equivalently,

$$\max_{(x,t)\in\Omega_T} |S(x,t) - S_m(x,t)| \le \frac{q^{m+1}}{1-q} \max_{(x,t)\in\Omega_T} |V_0(x,t)|.$$

Proof. Since

$$S - S_m = \sum_{k=m+1}^{\infty} V_k,$$

we obtain

$$\|S - S_m\|_{\mathbb{B}} \le \sum_{k=m+1}^{\infty} \|V_k\|_{\mathbb{B}}.$$

From

$$\|V_k\|_{\mathbb{B}} \le q^k \|V_0\|_{\mathbb{B}},$$

it follows that

$$\|S - S_m\|_{\mathbb{B}} \le \|V_0\|_{\mathbb{B}} \sum_{k=m+1}^{\infty} q^k = \frac{q^{m+1}}{1-q}\|V_0\|_{\mathbb{B}}.$$

This proves the stated conditional truncation-error estimate. □

4. Application and simulation

In this section, we investigate the nonlinear temporal-fractional A-CE to demonstrate that the recommended methods can manage challenging nonlinear fractional order problems. The results are quite positive and demonstrate the efficacy of the discussed strategies. In the current framework, the fractional operator incorporates the nonlocal effect into the projected model and provides extra degrees of freedom. The numerical experiments provide computational evidence of the accuracy and convergence behavior of the truncated MGMLFM and TAM approximations for the fractional Allen-Cahn problem over the tested spatial, temporal, and fractional-order ranges. The results are compared with the available reference solutions and previously reported approximations under the tested conditions. Finally, we contend that the proposed method is extremely dependable and applicable to extensive study classifications using fractional-order nonlinear scientific ways, which enhances our comprehension of nonlinear compound phenomena in related scientific and innovative domains. For accuracy's sake, we could examine the fractional/classical order plots, which demonstrate the close relationship between the exact and obtained solutions.

4.1. Implementation of MGMLFM on A-CE

In this subsection, we investigate the analysis and numerical simulation of the fractional A-CE Eq (1.1) with the following IC:

$$\mathscr{W}(x,0) = \mathscr{W}_0(x) = \frac{1}{1+e^{\frac{-x}{\sqrt{2}}}}, \tag{4.1}$$

where at $\alpha = 1$ in Eq (1.1), the exact solution is stated as [5]

$$\mathscr{W}(x,t) = \frac{1}{1+e^{(-\frac{x}{\sqrt{2}}-\frac{3}{2}t)}}. \tag{4.2}$$

From the MGMLFM process, we seek the approximate solution of Eq (1.1) in the following form:

$$\mathscr{W}(x,t) = \sum_{n=0}^{\infty} \mathscr{W}_0(x)\lambda_n(x)\frac{t^{n\alpha}}{\Gamma(n\alpha+1)}, \tag{4.3}$$

where $\lambda_n(x)$ are independent coefficient functions and are recursively determined by substituting the above series into the fractional A-CE and equating the coefficients of equal powers of t^{α} such that $\lambda_0(x) = 1$.From Lemma 2.1 and Eq (4.3), we have the following:

$$\sum_{n=0}^{\infty}\left[\mathscr{W}_0(x)\lambda_{n+1}(x) - \frac{\partial^2(\mathscr{W}_0(x)\lambda_n(x))}{\partial x^2} + \mathscr{W}_0^3(x)C_n\Gamma(n\alpha+1) - \mathscr{W}_0(x)\lambda_n(x)\right]\frac{t^{n\alpha}}{\Gamma(n\alpha+1)} = 0, \tag{4.4}$$

where

$$C_n = \sum_{i=0}^{n}\sum_{j=0}^{n-i}\frac{\lambda_i(x)\lambda_j(x)\lambda_{n-i-j}(x)}{\Gamma(i\alpha+1)\Gamma(j\alpha+1)\Gamma((n-i-j)\alpha+1)}. \tag{4.5}$$

Then, the recurrence relation is given by the following:

$$\lambda_{n+1}(x) = \frac{\frac{\partial^2(\mathscr{W}_0(x)\lambda_n(x))}{\partial x^2} - \mathscr{W}_0^3(x)C_n\Gamma(n\alpha+1) + \mathscr{W}_0(x)\lambda_n(x)}{\mathscr{W}_0(x)}. \tag{4.6}$$

Based on Eq (4.1), $\lambda_0(x) = 1$, and for $n > 0$, we have the following:

$$\lambda_1(x) = \frac{3}{2e^{\frac{x}{\sqrt{2}}} + 2},$$

$$\lambda_2(x) = -\frac{9(e^{\frac{x}{\sqrt{2}}} - 1)}{4(e^{\frac{x}{\sqrt{2}}} + 1)^2},$$

$$\lambda_3(x) = \frac{27\left(\left(-3e^{\frac{x}{\sqrt{2}}} + e^{\frac{3x}{\sqrt{2}}} + e^{\sqrt{2}x} + 1\right)\Gamma(\alpha+1)^2 - 2e^{\sqrt{2}x}\Gamma(2\alpha+1)\right)}{8\left(e^{\frac{x}{\sqrt{2}}} + 1\right)^4\Gamma(\alpha+1)^2}.$$

Additionally, by substituting various values of n, we can find the other factors, and by substituting in Eq (4.3), we get the solution in the following power series formula:

$$\mathscr{W}(x,t) = \mathscr{W}_0(\lambda_0(x) + \lambda_1(x)\frac{t^\alpha}{\Gamma(\alpha+1)} + \lambda_2(x)\frac{t^{2\alpha}}{\Gamma(2\alpha+1)} + \lambda_3(x)\frac{t^{3\alpha}}{\Gamma(3\alpha+1)} + \cdots).$$

These theoretical results are numerically simulated in the following figures and tables. All numerical computations reported in tables and plotted figures were performed using Wolfram Mathematica 12. The hardware used for runtime measurements is as follows: Intel Core i7-10750H CPU @ 2.60 GHz, 16 GB RAM, Windows 10 Pro 64-bit.

In Figure 1, we compare the precise classical solution in Eq (4.2) through 2D and 3D plots with the behavior of the four-term MGMLFM approximation at $\alpha = 1$ for $\mathscr{W}(x,t)$ in Eq (1.1). The approximate and exact solutions exhibit similar overall spatial-temporal behaviors, although the finite-term approximation does not exactly coincide exactly with the exact solution at all points. This observation is consistent with the fact that the displayed MGMLFM solution is a truncated four-term approximation. Additionally, we observe that the solution behavior for $\mathscr{W}(x,t)$ grows when we raise x and t. Figures 2 and 3 illustrate the effect of the fractional order α on the solution behavior. The profiles systematically change as α varies from 0.9, 0.7, and 0.5, indicating the influence of the fractional-order parameter on the temporal evolution of the solution.

In Table 1, we provide approximate numerical values acquired by the MGMLFM (current results) compared with exact values. Additionally, we offer a comparison of the estimated absolute errors for the A-CE problem (1.1) between the proposed method with the HPM and NITM published in [5] at diverse values of t when $\alpha = 1$ and $x = 1$. In Table 2, we compare the absolute errors resulting from analyzing several different methods published in the literature [6] under the conditions stated therein. From the table's data, it is evident that the approximate solutions have a high degree of agreement with the exact solution. Additionally, when compared to other previously published approaches, the absolute error calculated by the MGMLFM is extremely minimal.

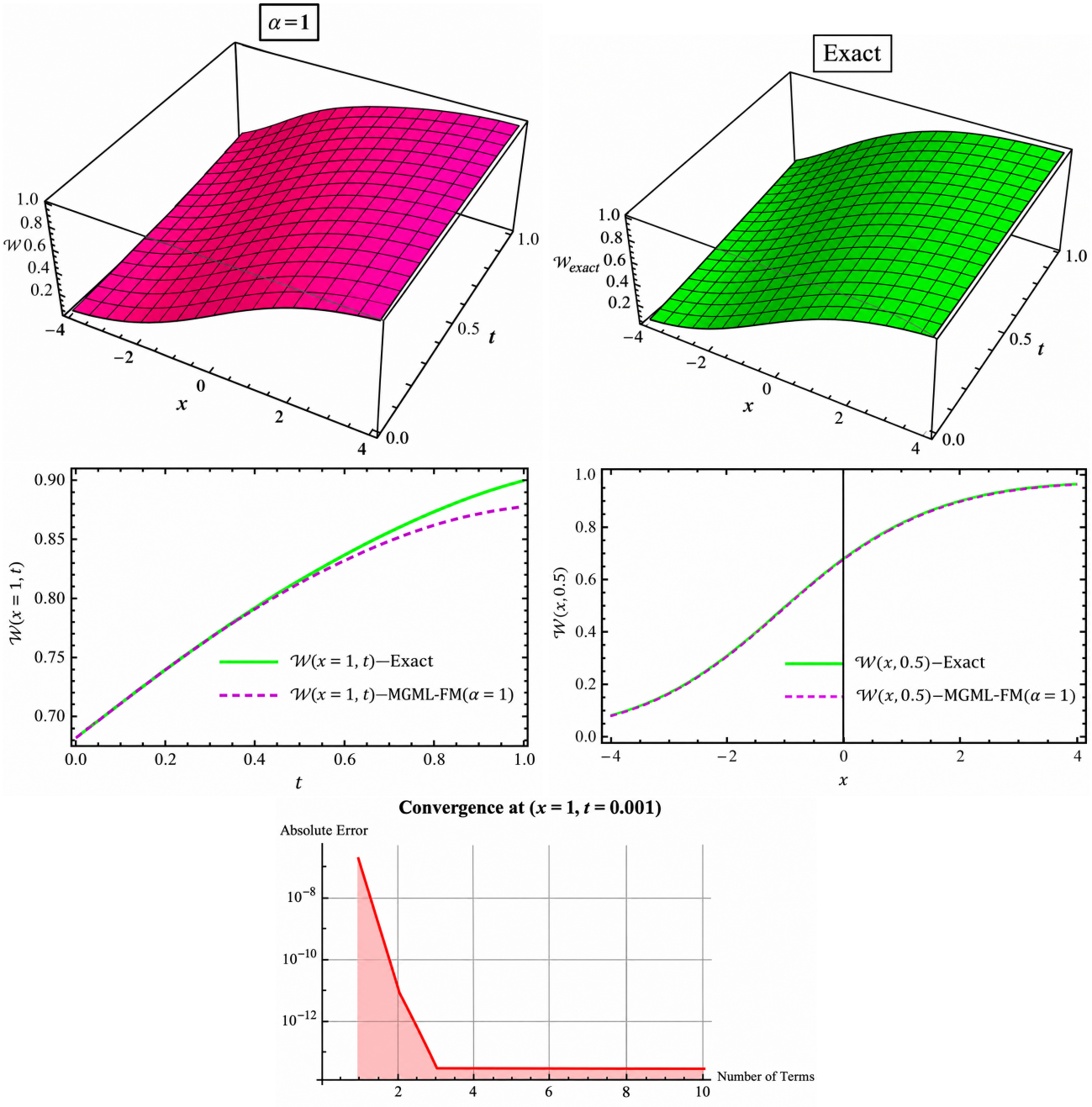


Figure 1. The 3D and 2D behavior of the MGMLFM approximate solution (four-term fractional series) when $\alpha = 1$ and the exact solution of $\mathcal{W}(x,t)$ in Problem (1.1). The 2D plot at $t = 0.5$ with a spatial range of $x \in [-4,4]$ and at $x = 1$ with a temporal range of $t \in [0,1]$.

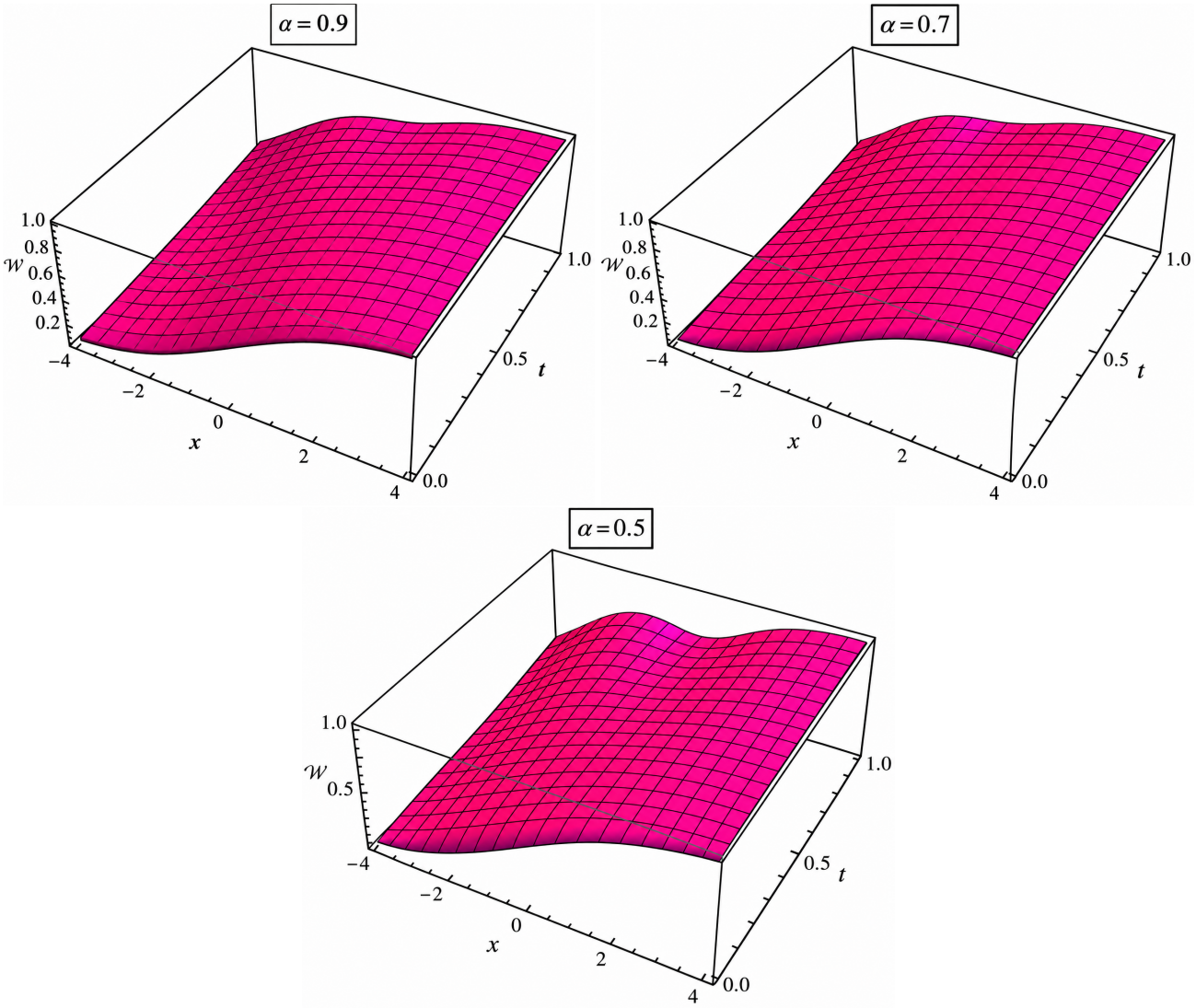


Figure 2. Behavior of the MGMLFM approximate solution (four-term fractional series) for $\mathscr{W}(x,t)$ in Problem (1.1) at different values of $\alpha = 0.9, 0.7, 0.5$ with a spatial range of $x \in [-4, 4]$ and a temporal range of $t \in [0, 1]$.

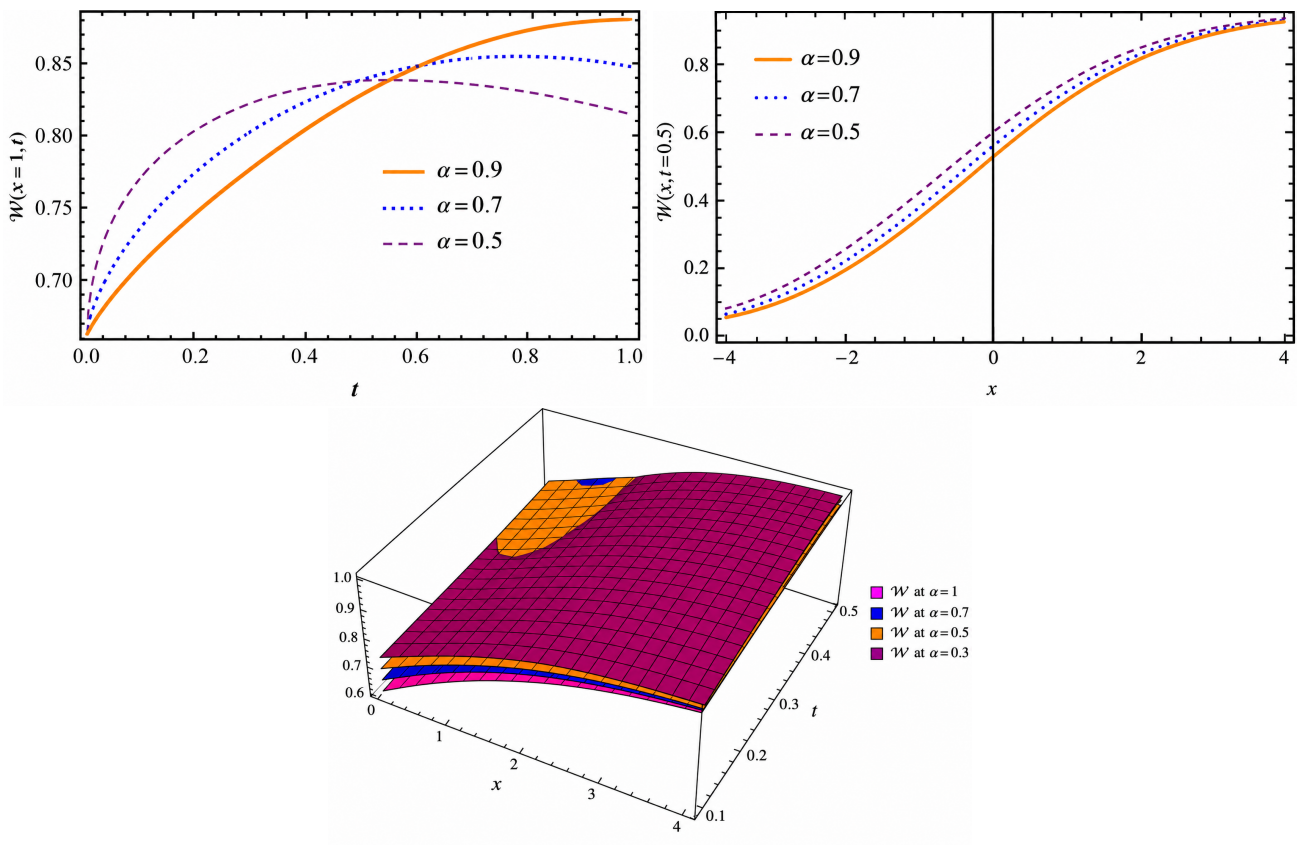


Figure 3. The 2D and 3D behavior of the MGMLFM approximate solution (four-term fractional series) for $\mathcal{W}(x,t)$ in Problem (1.1) at various values of $\alpha = 0.9, 0.7, 0.5$ with a spatial range of $x \in [-4, 4]$ and a temporal range of $t \in [0, 1]$.

Table 1. Approximate and exact values for A-CE (1.1) when $\alpha = 1$, with a comparison of absolute errors obtained by the MGMLFM (current results), HPM [5], and NITM [5] at $x = 1$ and various values of t.

t	MGMLFM solution	Exact	MGMLFM Abs.error	HPM Abs.error	NITM Abs.error
0.001	0.670093	0.670093	2.62013×10^{-14}	1.0×10^{-6}	3.3×10^{-11}
0.002	0.670425	0.670425	4.19331×10^{-13}	1.0×10^{-5}	2.6×10^{-10}
0.003	0.670756	0.670756	2.12341×10^{-12}	9.0×10^{-5}	8.9×10^{-10}
0.004	0.671087	0.671087	6.71141×10^{-12}	2.5×10^{-6}	2.1×10^{-9}
0.005	0.671418	0.671418	1.63871×10^{-11}	4.7×10^{-6}	4.1×10^{-9}
0.006	0.671749	0.671749	3.39846×10^{-11}	8.6×10^{-6}	7.1×10^{-9}
0.007	0.67208	0.67208	6.2968×10^{-11}	1.3×10^{-6}	1.1×10^{-8}
0.008	0.67241	0.67241	1.07434×10^{-10}	2.0×10^{-6}	1.7×10^{-8}
0.009	0.672741	0.672741	1.72109×10^{-10}	2.9×10^{-6}	2.4×10^{-8}
0.01	0.673071	0.673071	2.62353×10^{-10}	4.0×10^{-6}	3.3×10^{-8}

Table 2. Comparison between numerical errors of the proposed MGMLFM approximation at $\alpha = 1$ and other published methods [6]. All values are evaluated at $t = 0.0002$ over the spatial domain $x \in [0, 1]$, using the four-term approximation $\mathscr{W}^{[4]}$.

x	Abs.error (EITM)	Abs.error (NIM)	Abs.error (LRPSM)	Abs.error (MGMLFM)
0.0	7.5×10^{-6}	8.78908×10^{-12}	8.12989×10^{-16}	0
0.1	7.49063×10^{-6}	8.745×10^{-12}	3.3281×10^{-13}	1.11022×10^{-16}
0.2	7.46262×10^{-6}	8.61389×10^{-12}	7.02822×10^{-13}	0
0.3	7.41625×10^{-6}	8.39917×10^{-12}	1.10362×10^{-12}	0
0.4	7.35197×10^{-6}	8.10463×10^{-12}	1.52819×10^{-12}	0
0.5	7.27042×10^{-6}	7.73659×10^{-12}	1.96837×10^{-12}	1.11022×10^{-16}
0.6	7.17237×10^{-6}	7.30238×10^{-12}	2.41631×10^{-12}	0
0.7	7.05875×10^{-6}	6.81077×10^{-12}	2.86373×10^{-12}	1.11022×10^{-16}
0.8	6.9306×10^{-6}	6.27054×10^{-12}	3.30329×10^{-12}	1.11022×10^{-16}
0.9	6.78908×10^{-6}	5.692×10^{-12}	3.7277×10^{-12}	1.11022×10^{-16}
1.0	6.63542×10^{-6}	5.08504×10^{-12}	4.13074×10^{-12}	1.11022×10^{-16}

4.2. Applying TAM on A-CE

According to the TAM algorithm given in Subsection 3.2, the solution $\mathscr{W}(x,t)$ given in Eq (1.1) with the IC Eq (4.1) after applying $\mathcal{I}_t^\alpha$ to both sides are given as follows:

$$\mathscr{W}_{n+1}(x,t) = \mathscr{W}_0(x) + \mathcal{I}_t^\alpha \left[\frac{\partial^2 \mathscr{W}_n(x,t)}{\partial x^2} - \mathscr{W}_n^3(x,t) + \mathscr{W}_n(x,t) \right].$$

The initial iteration is as follows:

$$\mathscr{W}_0(x,t) = \frac{1}{1 + e^{\frac{-x}{\sqrt{2}}}}.$$

The next iteration is given as follows:

$$\mathscr{W}_1(x,t) = \mathscr{W}_0(x,t) + \mathcal{I}_t^\alpha \left[\frac{\partial^2 \mathscr{W}_0(x,t)}{\partial x^2} - \mathscr{W}_0^3(x,t) + \mathscr{W}_0(x,t) \right],$$

$$\mathscr{W}_1(x,t) = \mathscr{W}_0(x,t) + \frac{t^\alpha}{\Gamma(\alpha+1)} \left[\frac{\partial^2 \mathscr{W}_0(x,t)}{\partial x^2} - \mathscr{W}_0^3(x,t) + \mathscr{W}_0(x,t) \right].$$

The subsequent iteration is as follows:

$$\mathscr{W}_2(x,t) = \mathscr{W}_0(x,t) + \mathcal{I}_t^\alpha \left[\frac{\partial^2 \mathscr{W}_1(x,t)}{\partial x^2} - \mathscr{W}_1^3(x,t) + \mathscr{W}_1(x,t) \right].$$

Similarly, for $n \geq 2$ iterations, we can compute higher-order components and obtain the solution to Eq (1.1) as follows:

$$\mathscr{W}_{approx}(x,t) = \lim_{n \to \infty} \mathscr{W}_n(x,t) \approx \mathscr{W}_4(x,t). \tag{4.7}$$

The simulation of the TAM solution for the nonlinear time-fractional A-CE Eq (1.1) is presented in the following figures and tables. This iterative scheme starts from the IC and successively improves the approximate solution. The figures demonstrate the accuracy, convergence, and sensitivity to the fractional order α. Figure 4 shows 3D and 2D plots to compare the TAM approximate solution (using 4 iterations) when $\alpha = 1$ with the known exact solution Eq (4.2). The graphical profiles show close agreement between the two solutions over the displayed domain. Figure 5 displays the behavior of the TAM approximate solution at various fractional orders ($\alpha = 0.9, 0.8, 0.7$). The lower the value of α, the stronger the memory; therefore, past states have a greater impact on the present and resist rapid changes. The solution profiles vary as α changes from 0.9 to 0.7, illustrating the sensitivity of the temporal evolution to the fractional order. Figure 6 exhibits a comparison of the approximate solution across multiple α, highlighting the effect of fractional order on the solution dynamics in both 2D and 3D plots. Tables 3 and 4 provide a comparison between the TAM successive approximations $\mathscr{W}_1$, $\mathscr{W}_2$, $\mathscr{W}_3$, and $\mathscr{W}_4$ with the exact solution and compute absolute errors at each iteration. In Table 3, the time $t = 0.001$ is fixed and the spatial x varies from 0 to 1. The TAM solution converges extremely quickly — only 4 iterations are needed to achieve near-exact solutions (errors at machine zero). The method is spatially robust, handling both flat regions ($x = 0$) and steep gradient regions ($x = 1$) equally well after sufficient iterations. In Table 4, the position $x = 1$ is fixed and time t varies from 0.001 to 0.01. The TAM rapidly converges in time and space. The method is temporally consistent, as errors remain tiny across the entire time range studied. For four TAM iterations, the computed error remains of the order of 10^{-13} over the reported time interval. For example, the errors are 1.59761×10^{-13} at $t = 0.009$ and 2.74447×10^{-13} at $t = 0.01$,which is far superior to many other methods (compare with Table 1 where HPM errors are 10^{-6}). In addition, Table 5 provides a direct comparison between the proposed methods (four-term MGMLFM and four iterations TAM) approximate solutions and the previously published HAM results [7] for representative fractional orders. In particular, the cases $\alpha = 0.5$ and $\alpha = 0.75$ are considered at several spatial and temporal points. The close agreement between the two independent analytical approaches provides a literature-based cross-check of the fractional approximations. The case $\alpha = 1$ is presented separately because an exact classical solution is available for this limiting case. Therefore, the agreement at $\alpha = 1$ is only interpreted as a consistency check and is not used as a reference for the fractional cases $0 < \alpha < 1$.

The fractional order parameter α in the CFD plays a crucial physical role in the phase-separation dynamics modeled by the A-CE. It quantifies the degree of memory effects in the system: $\alpha = 1$ corresponds to the classical limit with no memory, where the system evolves based solely on its instantaneous state, $0 < \alpha < 1$ indicates the presence of memory, meaning that past configurations influence the current rate of phase evolution. Smaller values of α lead to stronger memory effects, resulting in slower kinetics, more diffuse interfaces, and smoother transitions from the IC to the equilibrium state. This behavior is clearly observed in our results (Figures 2, 3, 5, and 6), where decreasing α significantly retards the phase-separation process while preserving the same equilibrium phases. Physically, the fractional order α can be interpreted in terms of viscoelasticity (smaller α corresponds to more rubbery or glassy behavior), anomalous diffusion (subdiffusion for $\alpha < 1$), or the distribution of relaxation times in disordered or heterogeneous materials. Importantly, α affects the kinetics, not the thermodynamics, of phase separation—the driving force remains the same double-well potential, but the pathway to equilibrium is modified by memory effects. This makes the fractional A-CE a powerful framework to model real materials where atomic diffusion, viscoelastic response, or

microstructural history plays a significant role in the evolution of the phase morphology.

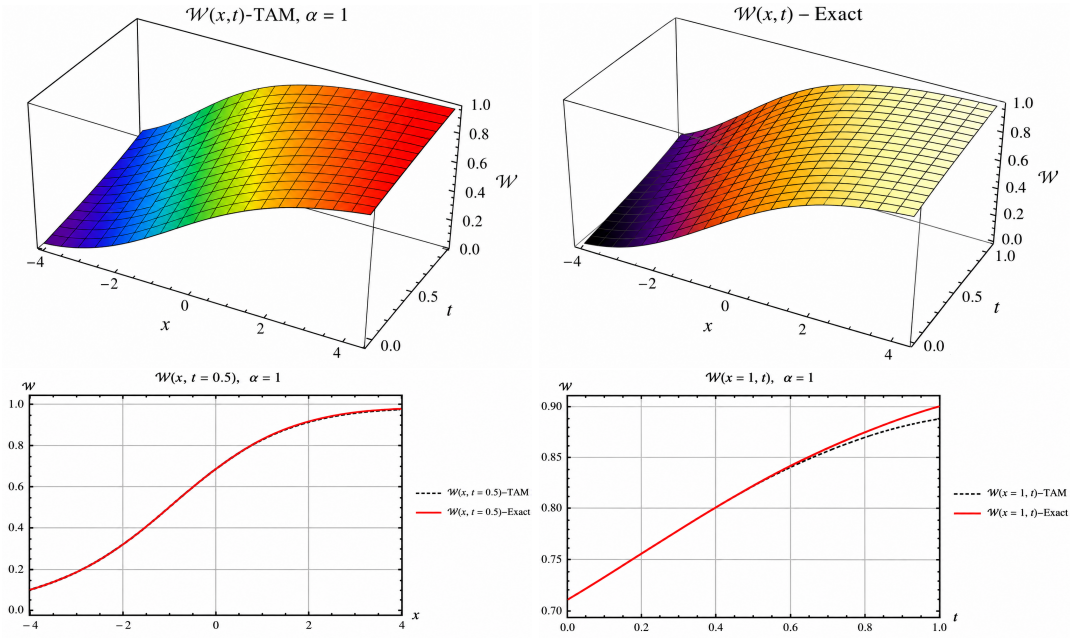


Figure 4. The 3D and 2D behavior of the TAM approximate solution (4 iterations) when $\alpha = 1$ and the exact solution of $\mathscr{W}(x,t)$ in Problem (1.1). The 2D plot at $t = 0.5$ with a spatial range of $x \in [-4, 4]$ and at $x = 1$ with a temporal range of $t \in [0, 1]$.

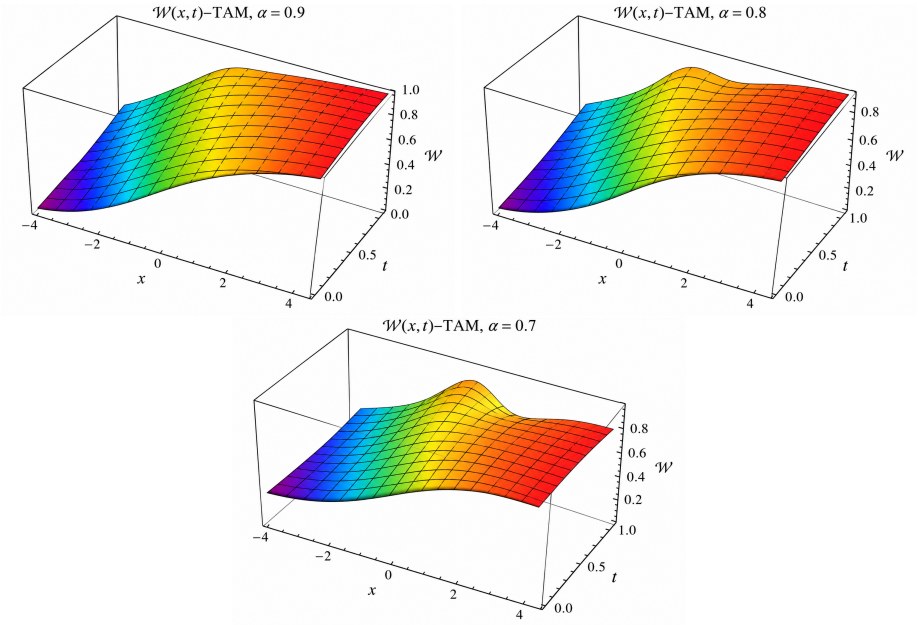


Figure 5. The behavior of the TAM approximate solution (4 iterations) for $\mathscr{W}(x,t)$ in Problem (1.1) at $\alpha = 0.9, 0.8, 0.7$ with a spatial range of $x \in [-4, 4]$ and a temporal range of $t \in [0, 1]$.

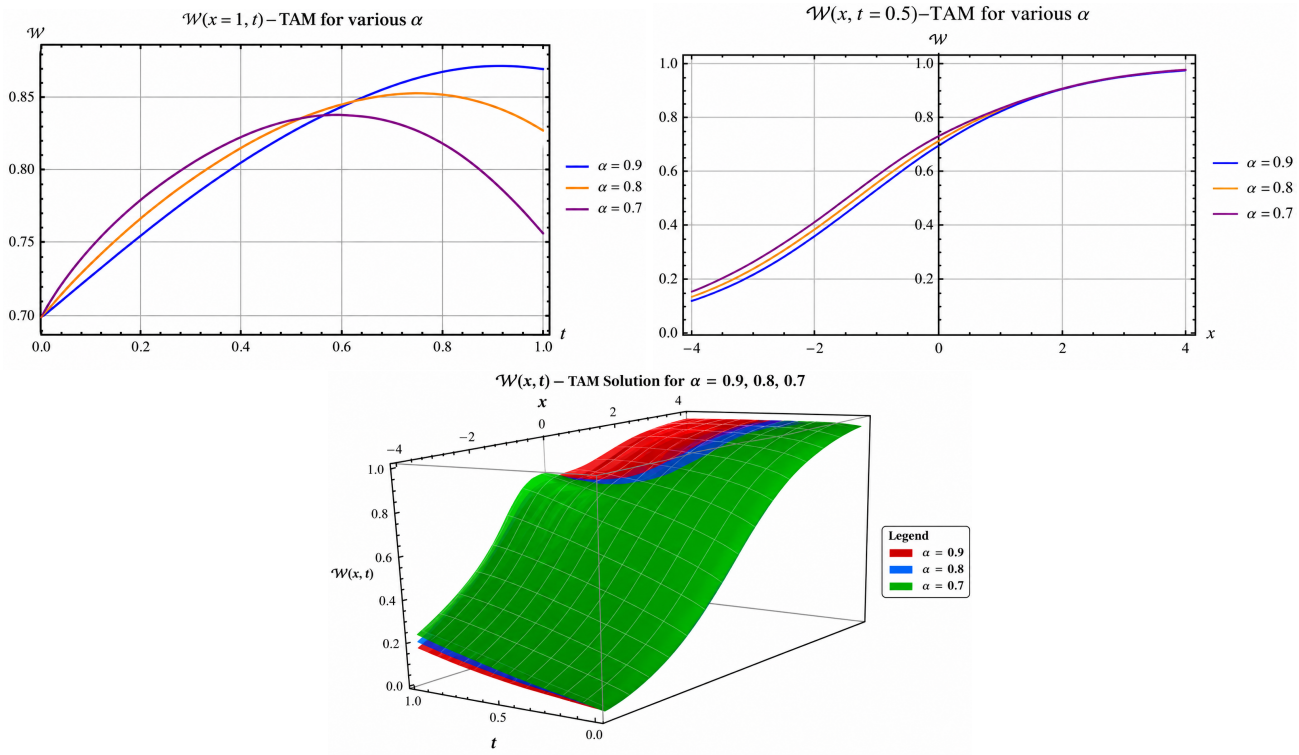


Figure 6. The 2D and 3D behavior of the TAM approximate solution (4 iterations) for $\mathscr{W}(x,t)$ in Problem (1.1) at various values of $\alpha = 0.9, 0.8, 0.7$ with a spatial range of $x \in [-4,4]$ and a temporal range of $t \in [0,1]$. The 2D plot at $t = 0.5$ with a spatial range of $x \in [-4,4]$ and at $x = 1$ with a temporal range of $t \in [0,1]$.

Table 3. Comparison of TAM four iterations with the exact solution and corresponding absolute errors at $t = 0.001$, $\alpha = 1$, and various x.

x	$\mathscr{W}_E xact$	$\mathscr{W}_1$	$\mathscr{W}_2$	$\mathscr{W}_3$	$\mathscr{W}_4$	$\lvert\mathscr{W}_E xact - \mathscr{W}_1\rvert$	$\lvert\mathscr{W}_E xact - \mathscr{W}_2\rvert$	$\lvert\mathscr{W}_E xact - \mathscr{W}_3\rvert$	$\lvert\mathscr{W}_E xact - \mathscr{W}_4\rvert$
0	0.500375	0.500375	0.500375	0.500375	0.500375	7.031253×10^{-11}	1.321165×10^{-14}	8.770762×10^{-15}	0
0.1	0.518045	0.518045	0.518045	0.518045	0.518045	9.997092×10^{-9}	2.670975×10^{-12}	7.771561×10^{-15}	0
0.2	0.53567	0.53567	0.53567	0.53567	0.53567	1.982427×10^{-8}	5.631939×10^{-12}	6.550316×10^{-15}	2.22045×10^{-16}
0.3	0.553206	0.553206	0.553206	0.553206	0.553206	2.945503×10^{-8}	8.841261×10^{-12}	4.996004×10^{-15}	1.33227×10^{-15}
0.4	0.570611	0.570611	0.570611	0.570611	0.570611	3.879671×10^{-8}	1.223899×10^{-11}	3.108624×10^{-15}	1.11022×10^{-16}
0.5	0.587842	0.587843	0.587842	0.587842	0.587842	4.776258×10^{-8}	1.576206×10^{-11}	1.332268×10^{-15}	2.10942×10^{-15}
0.6	0.604862	0.604862	0.604862	0.604862	0.604862	5.62736×10^{-8}	1.934575×10^{-11}	5.551115×10^{-16}	2.22045×10^{-15}
0.7	0.621631	0.621631	0.621631	0.621631	0.621631	6.425964×10^{-8}	2.292644×10^{-11}	2.553513×10^{-15}	3.44169×10^{-15}
0.8	0.638113	0.638114	0.638113	0.638113	0.638113	7.166084×10^{-8}	2.644329×10^{-11}	4.440892×10^{-15}	2.22045×10^{-15}
0.9	0.654278	0.654278	0.654278	0.654278	0.654278	7.842811×10^{-8}	2.983935×10^{-11}	6.328271×10^{-15}	8.88178×10^{-16}
1	0.670093	0.670093	0.670093	0.670093	0.670093	8.452374×10^{-8}	3.306344×10^{-11}	8.215650×10^{-15}	4.44089×10^{-15}

Table 4. Comparison of TAM four iterations with the exact solution and corresponding absolute errors at $x = 1$, $\alpha = 1$, and various t.

t	$\mathscr{W}_E xact$	$\mathscr{W}_1$	$\mathscr{W}_2$	$\mathscr{W}_3$	$\mathscr{W}_4$	$\lvert\mathscr{W}_E xact - \mathscr{W}_1\rvert$	$\lvert\mathscr{W}_E xact - \mathscr{W}_2\rvert$	$\lvert\mathscr{W}_E xact - \mathscr{W}_3\rvert$	$\lvert\mathscr{W}_E xact - \mathscr{W}_4\rvert$
0.001	0.670093	0.670093	0.670093	0.670093	0.670093	8.452374×10^{-8}	3.306344×10^{-11}	8.215650×10^{-15}	4.44089×10^{-15}
0.002	0.670425	0.670425	0.670425	0.670425	0.670425	3.382574×10^{-7}	2.647896×10^{-10}	1.328937×10^{-13}	4.44089×10^{-15}
0.003	0.670756	0.670757	0.670756	0.670756	0.670756	7.614443×10^{-7}	8.946196×10^{-10}	6.745715×10^{-13}	3.77476×10^{-15}
0.004	0.671087	0.671089	0.671087	0.671087	0.671087	1.354327×10^{-6}	2.122842×10^{-9}	2.137179×10^{-12}	1.77636×10^{-15}
0.005	0.671418	0.67142	0.671418	0.671418	0.671418	2.117147×10^{-6}	4.150597×10^{-9}	5.230372×10^{-12}	3.88578×10^{-15}
0.006	0.671749	0.671752	0.671749	0.671749	0.671749	3.050147×10^{-6}	7.179871×10^{-9}	1.087175×10^{-11}	1.68754×10^{-14}
0.007	0.67208	0.672084	0.67208	0.67208	0.67208	4.1535657×10^{-6}	1.141350×10^{-8}	2.018963×10^{-11}	4.18554×10^{-14}
0.008	0.67241	0.672416	0.67241	0.67241	0.67241	5.427645×10^{-6}	1.705518×10^{-8}	3.452494×10^{-11}	8.63754×10^{-14}
0.009	0.672741	0.672747	0.672741	0.672741	0.672741	6.872623×10^{-6}	2.430944×10^{-8}	5.543399×10^{-11}	1.59761×10^{-13}
0.01	0.673071	0.673079	0.673071	0.673071	0.673071	8.488739×10^{-6}	3.338168×10^{-8}	8.469137×10^{-11}	2.74447×10^{-13}

Table 5. Comparison of the four-term MGMLFM and four-iterations TAM approximate solutions with the previously published HAM results [7] for representative fractional orders $\alpha = 0.5$ and $\alpha = 0.75$, together with the classical case $\alpha = 1$, at different values of x and t.

t	x	$\alpha = 0.5$			$\alpha = 0.75$			$\alpha = 1.0$			
		HAM [7]	MGMLFM	TAM	HAM [7]	MGMLFM	TAM	MGMLFM	TAM	HAM [7]	Exact
0.25	0.2	0.720644	0.712333	0.720715	0.670868	0.669604	0.670498	0.626268	0.626315	0.626257	0.626311
	0.4	0.746049	0.737486	0.74324	0.700739	0.699334	0.700299	0.658709	0.658778	0.658755	0.658776
	0.6	0.770000	0.761698	0.764448	0.728997	0.727534	0.728495	0.689731	0.689817	0.689823	0.689817
	0.8	0.792442	0.784863	0.784647	0.755527	0.754085	0.754978	0.71914	0.719235	0.719263	0.719238
	1.0	0.813346	0.806857	0.804005	0.780257	0.778904	0.779683	0.746788	0.746888	0.746931	0.746892
0.50	0.2	0.773627	0.746499	0.76424	0.747948	0.739951	0.747236	0.708309	0.747236	0.710231	0.709183
	0.4	0.794027	0.76602	0.765455	0.772052	0.763506	0.770041	0.736254	0.770041	0.738428	0.737467
	0.6	0.813440	0.786266	0.768353	0.794543	0.785903	0.791239	0.762455	0.791239	0.764769	0.763915
	0.8	0.831778	0.806988	0.774598	0.815424	0.807118	0.811036	0.786858	0.811036	0.789202	0.788463
	1.0	0.848957	0.827805	0.784745	0.834708	0.827107	0.829572	0.80944	0.829572	0.811714	0.811090
0.75	0.2	0.801911	0.747647	0.742729	0.799847	0.777851	0.798041	0.774959	0.798041	0.782775	0.780130
	0.4	0.819719	0.763355	0.70577	0.818642	0.795083	0.808638	0.796799	0.808638	0.805400	0.803425
	0.6	0.837095	0.782152	0.679207	0.836326	0.812468	0.818865	0.817196	0.818865	0.826175	0.824807
	0.8	0.853776	0.803471	0.666699	0.852895	0.829951	0.829666	0.836216	0.829666	0.845168	0.844314
	1.0	0.869519	0.826482	0.668649	0.868329	0.847355	0.841467	0.853901	0.841467	0.862458	0.862013

5. Conclusions

This study employed two analytical approximation methods, namely the MGMLFM and the TAM, to obtain approximate analytical solutions for the nonlinear time-fractional A-CE, which models phase separation dynamics in iron alloys. The reliability and accuracy of proposed methods were assessed against the exact solution and compared with several existing approaches. The numerical outcomes were presented as tabulated values in Tables 1–4 and as graphical representations in Figures 1–6. The MGMLFM provides extremely high accuracy with very few terms in the series, while the TAM offers a straightforward iterative procedure that does not require recurrence relations or He's polynomials. These two methods produce small absolute errors, which are much less than those achieved by the HPM, NITM, EITM, LRPSM, and HAM, confirming their superior accuracy and reliability. Furthermore, for $\alpha \to 1$, the approximate solutions acquired using MGMLFM and TAM converge smoothly with the known exact solution of the classical A-CE, confirming the validity of the fractional model and the proposed methods. The 2D and 3D graphs show that the behavior of the solution

monotonically changes with α, reflecting the memory effects and long-range dependencies inherent in fractional systems, which highlights the flexibility of the fractional derivative in modeling complex physical phenomena. The results indicate that the MGMLFM and TAM are highly recommended for problems requiring high accuracy, and are preferred for quick and accurate estimations when computational simplicity is a priority. This study proves that these methods are powerful and easy-to-apply analytical tools for solving nonlinear fractional PDEs that arise in complex phenomena.

While the proposed MGMLFM and TAM demonstrate excellent performances for the problem under investigation, and while they offer significant advantages over existing methods in terms of accuracy and computational efficiency, the following limitations- like any other analytical method- should be honestly acknowledged to provide a balanced assessment of their scope and applicability. These limitations are that they only solve problems with ICs, provide more precise results in small time intervals, and an exact solution is needed for rigorous validation.

Future studies may expand these methods to include two-dimensional fractional systems, coupled equations, or models that involve other fractional derivative operators.

Author contributions

Conceptualization, H.M. Ali and W. Albalawi; Methodology, H.M. Ali; Validation, W. Albalawi and H.M. Ali; Formal analysis, H.M. Ali; Investigation, W. Albalawi; Resources, W. Albalawi and H.M. Ali; Software, H.M. Ali; Data curation, W. Albalawi; Visualization, W. Albalawi and H.M. Ali; Project administration, W. Albalawi; Funding acquisition, W. Albalawi; Writing—original draft, H.M. Ali; Writing—review and editing, H.M. Ali and W. Albalawi. All authors have read and agreed to the published version of the manuscript.

Use of Generative-AI tools declaration

The authors declare they have not used Artificial Intelligence (AI) tools in the creation of this article.

Acknowledgments

The research work was supported by Princess Nourah bint Abdulrahman University Researchers Supporting Project number (PNURSP2026R157), Princess Nourah bint Abdulrahman University, Riyadh, Saudi Arabia.

Conflict of interest

The authors declare that they have no known competing financial interests or personal relationships that could have appeared to influence the work reported in this paper.

References

1. H. Tariq, G. Akram, New traveling wave exact and approximate solutions for the nonlinear Cahn-Allen equation: evolution of a nonconserved quantity, *Nonlinear Dyn.*, **88** (2017), 581–594. https://doi.org/10.1007/s11071-016-3262-7

2. H. G. Lee, Y. Hwang, Y. Nam, S. Kim, J. Kim, Benchmark problems for physics-informed neural networks: the Allen-Cahn equation, *AIMS Math.*, **10** (2025), 7319–7338. https://doi.org/10.3934/math.2025335
3. M. M. A. Khater, A. R. Seadawy, D. Lu, Elliptic and solitary wave solutions for Bogoyavlenskii equations system, couple Boiti-Leon-Pempinelli equations system and time-fractional Cahn-Allen equation, *Results Phys.*, **7** (2017), 2325–2333. https://doi.org/10.1016/j.rinp.2017.06.049
4. G. Hariharan, K. Kannan, Haar wavelet method for solving Cahn-Allen equation, *Appl. Math. Sci.*, **3** (2009), 2523–2533.
5. L. Ali, R. Shah, W. Weera, Fractional view analysis of Cahn–Allen equations by new iterative transform method, *Fractal Fract.*, **6** (2022), 293. https://doi.org/10.3390/fractalfract6060293
6. I. Khan, R. Nawaz, A. H. Ali, A. Akgul, S. A. Lone, Comparative analysis of the fractional order Cahn-Allen equation, *Partial Differ. Equ. Appl. Math.*, **8** (2023), 100576. https://doi.org/10.1016/j.padiff.2023.100576
7. A. Esen, N. M. Yagmurlu, O. Tasbozan, Approximate analytical solution to time-fractional damped Burger and Cahn-Allen equations, *Appl. Math. Inf. Sci.*, **7** (2013), 1951–1956. https://doi.org/10.12785/amis/070533
8. H. Kim, Q. Jin, X. Wu, S. Kwak, Z. Li, J. Kim, An adaptive numerical method for solving the Allen–Cahn equation on curved surfaces, *J. Comput. Appl. Math.*, **486** (2026), 117702. https://doi.org/10.1016/j.cam.2026.117702
9. H. Kim, J. Ma, H. Shin, J. Kim, An efficient and accurate adaptive time-stepping method for the Allen–Cahn equation, *Comput. Math. Appl.*, **212** (2026), 62–77.https://doi.org/10.1016/j.camwa.2026.03.014
10. H. KIM, Numerical dynamics for the Allen–Cahn equation with variable mobility on curved surfaces, *J. Korean Soc. Ind. Appl. Math.*, **29** (2025), 360–376.
11. A. A. Kilbas, H. M. Srivastava, J. J. Trujillo, *Theory and applications of fractional differential equations*, Vol. 204, Amsterdam: Elsevier, 2006. https://doi.org/10.1016/S0304-0208(06)X8001-5
12. H. M. Ali, K. S. Nisar, W. R. Alharbi, M. Zakarya, Efficient approximate analytical technique to solve nonlinear coupled Jaulent–Miodek system within a time-fractional order, *AIMS Math.*, **9** (2024), 5671–5685. https://doi.org/10.3934/math.2024274
13. P. Agarwal, L. Vázquez Martínez, E. K. Lenzi, *Recent trends in fractional calculus and its applications*, Elsevier, 2024. https://doi.org/10.1016/C2022-0-00393-7
14. D. Baleanu, R. P. Agarwal, uFractional calculus in the sky, *Adv. Diff. Equ.*, **2021** (2021), 117. https://doi.org/10.1186/s13662-021-03270-7
15. A. A. M. Arafa, S. Z. Rida, H. Mohamed, Homotopy analysis method for solving biological population model, *Commun. Theor. Phys.*, **56** (2011), 797–800. https://doi.org/10.1088/0253-6102/56/5/01
16. D. D. Ganji, A. Sadighi, Application of homotopy-perturbation and variational iteration methods to nonlinear heat transfer and porous media equations, *J. Comput. Appl. Math.*, **207** (2007), 24–34. https://doi.org/10.1016/j.cam.2006.07.030

17. N. Iqbal, M. T. Chughtai, R. Ullah, Fractional study of the non-linear Burgers equations via a semi-analytical technique, *Fractal Fract.*, **7** (2023), 103. https://doi.org/10.3390/fractalfract7020103
18. M. Abbaszadeh, M. Dehghan, A reduced order finite difference method for solving space-fractional reaction-diffusion systems: the Gray-Scott model, *Eur. Phys. J. Plus*, **134** (2019), 620. https://doi.org/10.1140/epjp/i2019-12951-0
19. S. Tuluce Demiray, H. Bulut, F. B. M. Belgacem, Sumudu transform method for analytical solutions of fractional type ordinary differential equations, *Math. Probl. Eng.*, **2015** (2015), 131690. https://doi.org/10.1155/2015/131690
20. D. B. Dhaigude, G. A. Birajdar, Numerical solution of fractional partial differential equations by discrete Adomian decomposition method, *Adv. Appl. Math. Mech.*, **6** (2014), 107–119. https://doi.org/10.4208/aamm.12-m12105
21. O. P. Yadav, R. Jiwari, A finite element approach for analysis and computational modelling of coupled reaction diffusion models, *Numer. Meth. Partial Diff. Equ.*, **35** (2019), 830–850. https://doi.org/10.1002/num.22328
22. S. Javeed, D. Baleanu, A. Waheed, M. S. Khan, H. Affan, Analysis of homotopy perturbation method for solving fractional order differential equations, *Mathematics*, **7** (2019), 40. https://doi.org/10.3390/math7010040
23. H. M. Ali, Analytical investigation of the fractional nonlinear shallow-water model, *J. Appl. Math. Comput.*, **70** (2024), 5497–5514. https://doi.org/10.1007/s12190-024-02172-7
24. A. A. M. Arafa, S. Z. Rida, A. A. Mohammadein, H. M. Ali, Solving nonlinear fractional differential equation by generalized Mittag-Leffler function method, *Commun. Theor. Phys.*, **59** (2013), 661–663. https://doi.org/10.1088/0253-6102/59/6/01
25. J. Singh, D. Kumar, D. Baleanu, S. Rathore, An efficient numerical algorithm for the fractional Drinfeld-Sokolov-Wilson equation, *Appl. Math. Comput.*, **335** (2018), 12–24. https://doi.org/10.1016/j.amc.2018.04.025
26. H. Temimi, A. R. Ansari, A semi-analytical iterative technique for solving nonlinear problems, *Comput. Math. Appl.*, **61** (2011), 203–210. https://doi.org/10.1016/j.camwa.2010.10.042
27. I. Podlubny, *Fractional differential equations*, Mathematics in Sciences and Engineering, Vol. 198, San Diego: Academic Press, 1999. https://doi.org/10.1016/S0076-5392(99)X8001-5
28. D. Baleanu, K. Diethelm, E. Scalas, J. J. Trujillo, *Fractional calculus: models and numerical methods*, Series on Complexity, Nonlinearity and Chaos, Vol. 3, Singapore, New Jersey, London and Hong Kong: World Scientific Publishing Company, 2012. https://doi.org/10.1142/8180
29. H. Thabet, S. Kendre, J. Peters, Travelling wave solutions for fractional Korteweg-de Vries equations via an approximate-analytical method, *AIMS Math.*, **4** (2019), 1203–1222. https://doi.org/10.3934/math.2019.4.1203
30. A. Ghorbani, Beyond Adomian polynomials: He polynomials, *Chaos Soliton. Fract.*, **39** (2009), 1486–1492. https://doi.org/10.1016/j.chaos.2007.06.034



© 2026 the Author(s), licensee AIMS Press. This is an open access article distributed under the terms of the Creative Commons Attribution License (http://creativecommons.org/licenses/by/4.0)